

**CANADIAN NUCLEAR SOCIETY:
SIXTH INTERNATIONAL CONFERENCE ON CANDU FUEL**

**1999 September 26-30
Niagara Falls, Canada**

Sponsored/Supported by: Atomic Energy of Canada Limited, Cameco Corporation,
CANDU Owners Group, General Electric Canada, Hydro Quebec, International
Atomic Energy Agency, New Brunswick Power, STERN Laboratories Inc.
and Zircatec Precision Industries.

**CONFERENCE PROCEEDINGS
VOLUME 1**

R. Sejnoha, Editor

ORGANIZING COMMITTEE

Conference Chairman:	Roman Sejnoha
Conference Secretary:	Corneliu Manu & Parva Alavi
Program Chairman:	Mukesh Tayal
Program Secretary:	Paul Chan & Zoran Bilanovic
Facilities Coordinator:	Alan Manzer
Treasurer:	Peter Purdy
Registration:	Sylvie Caron & Daljit Rattan
Technical Tour Coordinator:	Fernando Doria
Publicity Coordinator:	Pamela Tume
Sponsorship:	Steve Palleck
Photographer:	Bernie Surette

Published by the Canadian Nuclear Society, 1999, Toronto
Copyright © Canadian Nuclear Society, 144 Front Street West, Suite 475, Toronto, Ontario, Canada, M5J 2L7
Contact: S. Caron, Tel: (416) 977-6152 ext.18; Fax: (416) 979 8356; e-mail: carons@cna.ca

**Vol 1: ISBN 0-919784-62-3
SET: ISBN 0-919784-64-X**

MEASUREMENT OF THE COMPOSITION OF NOBLE-METAL PARTICLES IN HIGH-BURNUP CANDU¹ FUEL BY WAVELENGTH DISPERSIVE X-RAY MICROANALYSIS

W.H. HOCKING AND F.J. SZOSTAK

AECL, Chalk River Laboratories, Chalk River, Ontario, CANADA K0J 1J0

ABSTRACT

An investigation of the composition of the metallic inclusions in CANDU fuel, which contain Mo, Tc, Ru, Rh and Pd, has been conducted as a function of burnup by wavelength dispersive X-ray (WDX) microanalysis. Quantitative measurements were performed on micrometer sized particles embedded in thin sections of fuel using elemental standards and the ZAF method. Because the fission yields of the noble metals change with burnup, as a consequence of a shift from almost entirely ²³⁵U fission to mainly ²³⁹Pu fission, their inventories were calculated from the fuel power histories using the WIMS-ORGIN code for comparison with experiment. Contrary to expectations that the oxygen potential would be buffered by progressive Mo oxidation, little evidence was obtained for reduced incorporation of Mo in the noble-metal particles at high burnup. These surprising results are discussed with respect to the oxygen balance in irradiated CANDU fuels and the likely intrinsic and extrinsic sinks for excess oxygen.

1. INTRODUCTION

Oxygen potential, which is directly correlated with stoichiometry, has been recognized as the most important chemical property of oxide nuclear fuels [1-5]. Thermal conductivity of the fuel is degraded by hyperstoichiometry, which in turn can cause higher than expected operating temperatures [6-8]. A small degree of hyperstoichiometry also increases thermal lattice diffusion rates of fission products by as much as several orders of magnitude through enhancement of the uranium vacancy population [2,9-12]. Furthermore, the valence state of several key fission products changes over the accessible range of oxygen potentials, with profound implications for their segregation behaviour [1,2,13,14].

All as-fabricated UO₂ fuels are probably at least slightly hyperstoichiometric, whereas (U,Pu)O₂ fuels can be significantly hypostoichiometric [1-5]. Because the effective mean valence of the fission products is less than two, some oxygen is expected to be freed during irradiation. Owing to a higher yield of the noble metals, plutonium fission is more oxidizing than uranium fission, which may be almost neutral [1,2,15]. The impact of irradiation on UO₂ stoichiometry should therefore be greater for CANDU fuels with natural uranium (0.7% ²³⁵U) than enriched light-water reactor (LWR) fuels: fission of plutonium isotopes created by neutron absorption becomes progressively more important at high burnup in the former, whereas fission

¹ CANDU (CANada Deuterium Uranium) is a registered trademark of Atomic Energy of Canada Limited.

of ^{235}U predominates in the latter. Consumption of excess oxygen by the Zircaloy sheath could effectively maintain a very low oxygen potential in the fuel [16]; however, the CANLUB graphite layer on the interior sheath surface of CANDU fuels appears to act as a barrier to oxygen gettering by the Zircaloy, at least under normal operating conditions [17]. Furthermore, significant hyperstoichiometry at the UO_2 grain boundaries has been suggested as a possible explanation for pronounced grain pullout observed during metallographic preparation of samples from high-burnup CANDU fuels [17].

Metallic alloy inclusions, composed of Mo, Tc, Ru, Rh and Pd, have been identified in many irradiated oxide fuels and SIMFUEL (simulated high-burnup oxide fuel) [1,16,18-21]. These precipitates, which have a hexagonal close-packed structure, are known as the ϵ -phase. They are typically observed, by optical and scanning electron microscopy (SEM), as micrometer-sized particles attached to fission-gas bubbles at the fuel grain boundaries, although much smaller intragranular inclusions have also been identified by TEM [20]. It has been proposed that Mo serves to buffer the oxygen potential in irradiated oxide fuels by progressively reacting with any excess oxygen, whether present initially or freed by fission; this should then be reflected by a corresponding reduction in the relative proportion of Mo retained in the ϵ -phase [1,16,22]. Significant *in situ* oxidation of Mo within previously formed noble-metal particles seems unlikely and would be inconsistent with observed behaviour (below). Oxidized Mo also has low solubility in the UO_2 matrix and has been found in a variety of complex mixed oxide phases that can form at the fuel grain boundaries and within the element void space [1]. Extensive measurements by wavelength dispersive X-ray (WDX) microanalysis on $(\text{U,Pu})\text{O}_{2-x}$ fuels, irradiated to very high burnup in fast breeder reactors, have revealed continuously decreasing Mo concentrations in the ϵ -phase particles, consistent with the anticipated evolution of the oxygen potential and trend toward stoichiometry. A rather narrow range of compositions has been found for the Mo-rich ϵ -phase particles in irradiated LWR fuels, which can be attributed to the limited amount of excess oxygen produced through ^{235}U fission and oxygen gettering by the Zircaloy sheath [1,16]. Only a single qualitative examination of metallic particles extracted from irradiated CANDU fuel has been reported: Mo, Tc, Ru and Pd were identified, but any Rh present would have been masked by Ru in the low-resolution, energy dispersive X-ray (EDX) spectra [23].

A more systematic investigation of the composition of the noble-metal particles in CANDU fuels as a function of burnup was therefore undertaken by WDX microanalysis. Initially, X-ray spectra were recorded from particles adhering to fuel fragments obtained by crushing whole fuel pellets; these preliminary experiments were conducted to demonstrate the feasibility of analyzing the comparatively small noble-metal inclusions normally encountered in CANDU fuel. Quantitative measurements were then performed, using elemental standards and the ZAF method [24], on larger populations of particles embedded in metallographically prepared thin sections of fuel taken from different elements spanning a wide range of burnup. Because the fission yields of the noble metals change as a function of burnup, the total inventories of the five metals were calculated from the fuel power histories using the WIMS-ORIGEN code [25] for comparison with experiment. The results have been assessed with respect to the oxygen balance in irradiated CANDU fuel and the likely sinks for excess oxygen.

2. EXPERIMENTAL PROCEDURES

A Hitachi S-570 SEM equipped with a single Microspec four-crystal WDX spectrometer was used for the qualitative preliminary investigation of the noble-metal particles in irradiated CANDU fuel. This instrument is located directly above a hot cell at the AECL Whiteshell Laboratories (WL). All parts of the microscope that are necessarily exposed to high radiation fields, including the electron optics column, the sample analysis chamber and the WDX spectrometer, have been separated from the control/electronics console and installed within a lead-shielded enclosure [26]. Various other modifications were also made to facilitate remote operation and handling of highly radioactive materials, notably placement of lead sheets (outside the vacuum system) between the analysis chamber and the housing of the WDX spectrometer for additional shielding of the X-ray detector.

The shielded-SEM/WDX facility at the AECL Chalk River Laboratories (CRL) is similar in concept and layout to the WL system described above, but is based upon a JEOL 840A SEM with twin JEOL WDX spectrometers. Because of differences in instrument design, external shielding of the X-ray detectors was not possible in this case; instead, custom-made shield plates were fitted inside the vacuum system. The WDX spectrometers are controlled by a Tracor Northern TN5500 computer system that includes routines for quantitative analysis using the ZAF matrix correction procedure, according to the following equation:

$$C_x = C_s(I_x/I_s)ZAF \quad (1)$$

where C_x is the concentration of element x in the unknown, C_s is the known concentration of x in a standard; I_x is the X-ray intensity measured for x from the unknown, I_s is the comparable value determined from the standard; and Z , A and F are matrix correction factors related to differences in atomic number, X-ray absorption and X-ray fluorescence respectively [24,27].

Elemental standards were available for Mo, Ru, Rh, Pd and U, but not Tc; therefore, the concentration of Tc in the noble-metal particles was estimated using relative sensitivity factors derived from the measurements on Mo and Ru (which are the adjacent elements in the Periodic Table). The net X-ray signal intensities (I_x and I_s) required for Equation (1) were determined by an automated process that monitored the count rate on each peak and at an adjacent energy (background level subtracted). A 25 kV electron beam, with 40-50 nA of current, was normally used to excite the X-ray emission; experiments performed at other beam voltages (10-40 kV) and currents (15-60 nA) did not show any dependence of the noble-metal relative proportions obtained on the measurement conditions. Because of partial sampling of the fuel matrix, some uranium was invariably detected together with the noble metals. Typically, analysis of a particle ~2 μm in size would yield an absolute composition totaling 100 ± 10 wt.%, including ~5 wt.% uranium — proportionately larger amounts of U were found for smaller particles. The measurements were normally performed in triplicate to check for consistency and then averaged (until reproducibility had been established, some analyses were repeated up to 9 times). A number of WDX analyses of the fuel matrix under the same conditions did not reveal detectable levels of any of the noble metals.

Power histories and some other relevant information on the CANDU fuels that were the subject of the present investigation are provided in Table 1. Inventories of Mo, Tc, Ru, Rh and Pd calculated for these fuels are reported in Table 2 as proportions (in wt.%) of the total noble-metal content [25,28]. For the initial studies at WL, discrete fragments of fuel, typically ~4 mm in size, were selected from crushed whole pellets (only P11171W/7 and BDL-406-GF/2). Further details of the sampling methodology and secondary electron images of comparable fragments have been previously reported [14]. The original location of the fragment within the fuel pellet could be approximately inferred from the morphology. Rectangular, thin sections of fuel (~8 mm long, ~4 mm wide and ~1 mm thick) were prepared, using standard metallographic methods, for the quantitative measurements at CRL. The wafer was oriented perpendicular to the former pellet axis and the long dimension included a segment of sheath at one end; this allowed the radial location of any features to be determined. Surface charging during the electron beam interrogation was inhibited by sputter coating each mounted sample with a light film of carbon or gold (no difference was found in the results).

3. RESULTS

During the initial phase of this study, WDX spectra were recorded from noble-metal particles, typically ~1 μm in size, attached to fragments of the fuels with the lowest and highest burnup (Table 1). Although the exact radial location could not be specified, such particles were found only on fragments that originated from near the fuel centerline. Illustrative examples of the extremes of behaviour observed are displayed in Figures 1 and 2; all five of the ϵ -phase constituents have been identified here, although the Rh L_α peak is partly overlapped by the Ru L_β peak. For the low-burnup fuel (Figure 2), the relative intensities of the L_α peaks arising from the three main constituents are in qualitative agreement with the calculated inventories (Mo > Ru > Pd) reported in Table 2. Conversely, for the high-burnup fuel (Figure 1), the L_α peak of Pd is stronger than the corresponding peaks arising from Mo and Ru, by more than a factor of two, despite the fact that the inventories of the three elements are now comparable (Mo still largest, but by a small margin and Ru is nearly equal to Pd, Table 2). These preliminary results suggested confirmation of the expected trend of declining Mo participation in the ϵ -phase with increasing burnup; however, only a few Pd-rich particles were found and WDX spectra collected from other particles (on the high-burnup fuel fragments) revealed Pd levels comparable with or less than Ru and Mo (Figure 3).

During the second phase of this study, sectioned noble-metal particles embedded in polished wafers of fuel were quantitatively analyzed using the ZAF method as described above. A few WDX spectra were also recorded for comparison with the preliminary work; an illustrative example showing resolution of the Rh L_α and Ru L_β peaks has been reproduced in Figure 4. In all cases, noble-metal particles were identified only within a core region extending from the fuel centerline out to ~30% of the pellet radius — no compositional dependence on radial location was evident here. The measured compositions of 12 noble-metal particles found within the Bruce fuel J03311W/3 are reported (as wt.% of the 5 metals normalized to 100%) in Table 3. Because of the comparatively high power at which this fuel operated, the particles were sufficiently large (2-3 μm) to minimize sampling of the fuel matrix and even the minor

constituents could be precisely determined. The results for particles 1-8 are quite consistent, while particles 9-12 show some variability. Although the range of measured concentrations spans the calculated inventories (compare Table 2 and 3) for every element, there is closer agreement in general for Mo and Rh than Tc, Ru and Pd. The experimentally determined Mo/Ru ratio is ~15% below the predicted value on average, with only one individual measurement that is higher (for particle 9), which could suggest modest depletion of Mo from the noble-metal particles. Conversely, the measured Mo/Pd ratio is rather larger on average than calculated — despite the two low values for particles 11 and 12 — consistent with depletion of Pd rather than Mo from the ϵ -phase.

The results from quantitative WDX analyses of the noble-metal particles in the other three high-burnup fuels are reported in Table 4 as Mo/Ru and Mo/Pd ratios. For the two natural uranium fuels, the experimentally determined Mo/Ru ratios are generally in excellent agreement with the calculated inventories, whereas the Mo/Pd ratios are clearly larger than predicted in all but one case (particle 2 of J98315C/28). These ϵ -phase particles are thus deficient in Pd rather than Mo, which is contrary to the premise that fission-freed oxygen would be consumed by Mo oxidation at high burnup. A likely explanation for the lower than expected Pd content of most noble-metal particles in high-burnup CANDU fuel was provided by the measurements on the (U,Pu)O₂ fuel: in addition to the typical ϵ -phase particles, a couple of Pd-rich particles (7 and 9), containing only minor amounts of Mo and Ru, were found as well. These are undoubtedly the cubic α -phase particles that have been identified in SIMFUEL and fast breeder reactor fuels with very high burnup [1,21,29]. The formation of even a small population of α -phase particles would effectively reduce the average Pd content in the primary ϵ -phase and probably accounts for the initial result above from the UO₂ fuel with the highest burnup. Preferential relocation of Pd, which is less refractory than the other metals, away from the central region of the fuel is also possible and could therefore be a contributing factor [29]; however, as already noted, no correlation of particle composition with radial location was apparent.

4. DISCUSSION

The measured compositions of the noble-metal particles in irradiated CANDU fuels spanning a wide range of burnup thus provide little evidence of progressive Mo oxidation. This finding is in agreement with extensive studies of fission-product segregation by X-ray photoelectron spectroscopy (XPS): for intact elements, oxidized Mo has only rarely been detected (and then in low abundance) at either the UO₂ grain boundaries or the fuel-sheath interface [14,30,31]. Although contrary to expectations based on analogy with fast breeder reactor fuels, the oxygen potential in CANDU fuels would therefore appear to remain below the MoO₂/Mo boundary even at high burnup, which also implies that the bulk U_{1-y}Pu_yO₂ would remain only slightly hyperstoichiometric [1-3].

In order to better understand these surprising results, the oxygen balance in CANDU fuel was considered in further detail. Speciation of fission products was initially assumed to involve only binary compounds, either oxides or halides, and pure elements. The valence state of each fission product was then assigned (Table 5), according to known thermodynamic data, for oxygen

potentials either above or below the MoO_2/Mo boundary [1]. Next, the amount of oxygen released by fission was derived from the calculated fission-product inventories at normal and high burnup (top part of Table 6) [25,32]. For the normal-burnup fuel, all of the available oxygen could have been consumed solely through oxidation of Mo. Conversely, for the high-burnup fuel, because of the progressive impact of plutonium fission, even with complete Mo oxidation, a significant excess of oxygen would still be predicted. Clearly, this simple model is inadequate to account for the chemistry of irradiated CANDU fuel; more subtle aspects will now be considered, including both intrinsic and extrinsic sinks for oxygen.

The trivalent rare earths and yttrium (collectively denoted by RE) as well as Ce^{4+} all readily substitute for the U^{4+} ion in the uraninite lattice to relatively high concentrations [33-35]. Charge balance can be maintained either through hypostoichiometry, i.e., creation of oxygen vacancies giving $\text{RE}_y\text{U}_{1-y}\text{O}_{2-y/2}$, or by a matching increase in the average uranium valence, $\text{RE}_y\text{U}_{1-y}\text{O}_2$. Because of the stability of the stoichiometric uraninite structure, an O/M ratio of almost exactly two can be maintained to relatively low oxygen potentials for modest rare earth concentrations — the equivalent amount of U^{5+} and/or U^{6+} in UO_{2+x} would require a much higher oxygen potential [2,3,33-35]. An additional O^{2-} ion should therefore be bound in the fuel matrix for every two RE^{3+} ions, even somewhat below the MoO_2/Mo boundary (Table 6). The divalent alkaline earths (denoted AE) can substitute for U^{4+} in the uraninite lattice in a similar fashion to the rare earths, $\text{AE}_y\text{U}_{1-y}\text{O}_{2-z}$, and form separate uranate phases of the form AEUO_{4-z} [36,37]; Sr predominantly remains dispersed in the fuel matrix, whereas Ba commonly segregates to an appreciable extent [1,14,30,31]. In either case, the additional oxygen is likely bound less strongly than for rare earth lattice substitution, although the thermodynamics of the Ba-Sr-U-O system are not well known [37]. Significant segregation of Ba but not Sr to the grain boundaries and the fuel-sheath interface, has been routinely found in XPS studies of CANDU fuel; however, insufficient reference data are available to distinguish between the possible oxides and uranates [14]. Accordingly, the maximum amount of additional oxygen that could be bound by the alkaline earths (in the fuel matrix and uranate phases combined) has been multiplied in Table 6 by a coefficient ($\alpha < 1$) to allow for hypostoichiometry.

The monovalent alkali metals (Rb and Cs) have relatively low solubility in the uraninite structure and have been shown to preferentially segregate to the UO_2 grain boundaries and the fuel-sheath interface [1,2,14,31]. Numerous studies of the Cs-U-O system have indicated that complex phases of the generic form $\text{Cs}_2\text{UO}_{4-z}$ are stable for oxygen potentials near the MoO_2/Mo boundary [1,2,37,38]. The maximum additional oxygen that could be bound in such phases here, after allowing for reaction with the halides (i.e., formation of CsI, RbBr, etc.), has again been reported in Table 6; in this case, the range of possible values for the hypostoichiometry coefficient ($0.5 < \beta < 1$) would appear to be limited.

Three additional fission products that would be expected to remain in an elemental state, Sn, Cd and Te, are known to exhibit anomalous behaviour. Studies of fission-product segregation in CANDU fuel by XPS have identified only oxidized forms of Sn and Cd, whereas both elemental and oxidized Te have been found [14,30,31]. Because the SnO_2/Sn boundary lies just above that for MoO_2/Mo , oxidation of Sn can be accommodated by modest stabilization of elemental Mo when it is alloyed with more noble metals [39]. Conversely, oxidation of Cd and especially Te would require either much higher oxygen potentials (unlikely) or formation of more stable mixed

oxides (e.g., BaTeO_3 and CdTeO_3) about which not much is known [1,14]. Thus, there is considerable uncertainty in the value of the coefficient ($\gamma < 1$) multiplying the maximum amount of oxygen that could potentially be bound by these three elements in CANDU fuels (Table 6).

The amount of fission-freed oxygen predicted (Table 6) for the normal-burnup CANDU fuel, when the oxygen potential remains below the MoO_2/Mo boundary, could be entirely consumed by the intrinsic oxygen sinks discussed above, although somewhat optimistic values would be required for α , β and γ . Conversely, for the high-burnup fuel, the intrinsic oxygen sinks could accommodate at most $\sim 2/3$ of the calculated excess oxygen (with the oxygen potential below the MoO_2/Mo boundary) and realistic values for the coefficients reduce this to less than half. Extrinsic sinks for oxygen, involving the CANLUB layer and the Zircaloy sheath, must therefore be considered as well.

The CANLUB layer prevents stress-corrosion cracking of the thin-walled sheath on CANDU fuels by serving as a chemical barrier to fission products, especially iodine, but it appears also to inhibit reaction of any excess oxygen with the Zircaloy [17,40]. During the fuel fabrication, colloidal graphite together with an organic binder is applied to the sheath interior surface and then baked at over 300°C for several hours. Although the finished CANLUB layer consists predominantly of carbon, there are small proportions of hydrogen and oxygen present as well, in the form of organic compounds, which are rapidly destroyed by irradiation. The released hydrogen will either react with any available oxygen to form water or dissolve in the Zircaloy. The maximum amount of free hydrogen that could thus be introduced into the element (in excess of that needed to react with oxygen from the binder) was estimated from the initial formulation (Table 6). Because most of the organic binder is probably lost during the initial bake, the actual amount of hydrogen will almost certainly be much less ($\delta \ll 1$), hence the overall impact on the oxygen balance in the fuel should be insignificant. However, the formation of even trace quantities of water might partly explain indications of fuel degradation at high burnup [17] — full monolayer coverage of the entire UO_2 grain-boundary network could be provided by just 0.3 mmole of H_2O per element.

The carbon component of CANLUB is by comparison a potentially important extrinsic oxygen sink; a typical inventory of carbon in an element is thought to be ~ 200 mg, although the layer uniformity (3-10 μm thick) can vary considerably. Progressive disappearance of the CANLUB layer as a function of burnup has been well documented through post-irradiation examinations by optical and scanning electron microscopy [17]. Nonetheless, mass spectrometric analyses of the gas present in CANDU fuel elements after irradiation have consistently found only negligible amounts of CO and CO_2 even at high burnup. Recent studies by XPS and SEM/WDX have shown that carbon remains the most abundant element at the fuel-sheath interface; however, they have also confirmed that there is considerable redistribution of carbon and revealed significant incorporation of oxygen into the graphite at high burnup [31]. The calculated total carbon inventory has been reported in Table 6 with a multiplying factor of η , which has been estimated to approach ~ 0.3 for the BDL-406-GF fuel based upon chemical-shift effects for the C 1s peak [31]. This coefficient would undoubtedly have a smaller value for normal-burnup fuel, consistent with the limited XPS data available.

As the CANLUB layer becomes degraded with increasing burnup, conventional post irradiation examinations have revealed formation of a thin oxide film on the interior sheath surface, which has been identified as ZrO_2 by XPS analysis [17,31]. Growth of this film is characteristically nonuniform, with only patches of oxide being visible initially and the thickness ranging from $<1 \mu\text{m}$ to $>10 \mu\text{m}$ at the highest burnup. For the BDL-406-GF fuel, the oxygen consumed by ZrO_2 formation was calculated assuming an average film thickness of $3 \mu\text{m}$; the result is reported in Table 6 and represents a modest further contribution to the overall oxygen balance.

The incorporation of even a small proportion of oxygen into the CANLUB layer ($\eta \sim 0.1$) allows all of the calculated excess oxygen at normal burnup to be easily accommodated with realistic values for the other coefficients ($\alpha < 0.5$, $\beta \sim 0.5$ and $\gamma < 0.5$). In the case of the high-burnup fuel, however, the predicted amount of fission-freed oxygen (in the absence of Mo oxidation) is near the total capacity for all of the extrinsic and intrinsic sinks listed in Table 6 (per element, 69.7 mmole consumed with $\alpha = \beta = \gamma = \delta = \eta = 1$ versus 67.3 mmole liberated). If plausible values are chosen for the various coefficients, only $\sim 2/3$ of the calculated excess oxygen would be consumed. Dissolution of oxygen in the Zircaloy beneath the surface oxide film might be a partial explanation for the remainder. Significant concentrations of oxygen ($\sim 12 \text{ at.}\%$) have been found in LWR fuel sheaths (by WDX microanalysis) to depths of $\sim 20 \mu\text{m}$ from the surface, despite a fuel-sheath gap $\sim 20 \mu\text{m}$ wide that is partly filled with a complex ceramic phase consisting of mixed fission-product and zirconium oxides [16]. There are no data presently available on oxygen dissolution in CANDU fuel sheaths at high burnup, but it would seem unlikely that this sink could account for all of the difference above: assuming 12 at.% dissolved-oxygen concentration, a penetration depth of $\sim 140 \mu\text{m}$ would be needed.

The preceding discussion has implicitly assumed that thermodynamic equilibrium was achieved throughout the whole fuel matrix during the irradiation, which is clearly not the case. Internal energy released by fission maintains a steep temperature gradient across the fuel radius: the outer elements in a CANDU fuel bundle typically operate with centerline temperatures of $1200\text{-}1700^\circ\text{C}$ and periphery temperatures of $400\text{-}500^\circ\text{C}$. The noble-metal inclusions analyzed here were all located in the hot central part of the fuel, because the diffusion rates elsewhere are much too slow to allow formation of micrometer-sized particles [41]. In cooler regions of the fuel, fission products with low solubility in the UO_2 lattice, including the noble metals, will still precipitate at extended burnup, but then form tiny particles ($<30 \text{ nm}$ in size) that are dispersed throughout the grains as well as along the grain boundaries [20]. Conversely, oxygen mobility in the fuel is sufficiently high even at the periphery to ensure that a steady-state distribution is maintained (the oxygen diffusion rate in UO_{2+x} is 4-10 orders of magnitude larger than that of any other species and it can also migrate along cracks in the vapour phase) [41,42]. All of the metallic fission products, including Mo, have MO_x/M boundaries with large positive temperature coefficients (see for example Figure 2 in reference [1]); hence, conditions become significantly less oxidizing with increasing temperature for constant oxygen potential and even more so if the oxygen partial pressure is constant. Oxidation of Mo (and other fission products) in the cooler regions of the fuel, where segregation is too limited to allow practical analysis, might therefore account for the balance of the excess oxygen at high burnup (Table 6). However, measurements of oxygen redistribution in hyperstoichiometric $U_{1-y}Pu_yO_{2+x}$ fuels have indicated that it migrates up the thermal gradient, at least for temperatures above 1200°C [41,42], which should increase

the oxygen potential in the hot central region. Because the boundaries for MoO_2 and $\text{U}_{1-y}\text{Pu}_y\text{O}_{2+x}$ with $y < 0.03$ and $x \sim 0.001$ cross near 1400°C [1], there would still be some latitude for Mo to be appreciably oxidized in the cooler regions of the high-burnup CANDU fuel and largely metallic near the center.

5. CONCLUSIONS

Quantitative X-ray microanalyses of the noble-metal inclusions formed in the central region of CANDU fuels spanning a wide range of burnup have been performed. Comparison of the measured relative proportions of Mo, Ru and Pd in these particles with calculated fission-product inventories provided little evidence of Mo oxidation. This also implies that the $\text{U}_{1-y}\text{Pu}_y\text{O}_{2+x}$ matrix has remained nearly stoichiometric ($x < 0.001$) even at the highest burnup attained. Further evaluation of the possible intrinsic and extrinsic sinks for fission-freed oxygen has shown that all of it can be reasonably accounted for, except at the highest burnup where there is still some uncertainty in the fate of $\sim 1/3$ of the excess. Nonetheless, significantly greater capacity for buffering the oxygen potential in CANDU fuel has been revealed than was previously apparent.

6. ACKNOWLEDGEMENTS

The authors are grateful to R. Behnke for recording the initial WDX spectra using the Hitachi instrument located at the Whiteshell Laboratories. They would also like to thank G. Edwards for calculating the fission-product inventories in the three high-burnup CANDU fuels using the WIMS-ORIGEN code, and C.A. Buchanan for preparing the thin sections of fuel. Finally, the authors would like to thank R.A. Verrall, H.J. Matzke and H. Kleykamp for constructive review of the manuscript and helpful comments on the chemistry of irradiated nuclear fuels.

6. REFERENCES

1. KLEYKAMP H., "The Chemical State of the Fission Products in Oxide Fuels", J. Nucl. Mater. 131, 221-246 (1985).
2. GITTUS J.H., J.R. MATTHEWS and P.E. POTTER, "Safety Aspects of Fuel Behaviour During Faults and Accidents in Pressurised Water Reactors and in Liquid Sodium Cooled Fast -Breeder Reactors", J. Nucl. Mater. 166, 132-159 (1989).
3. LINDEMNER T.B. and T.M. BESMANN, "Chemical Thermodynamic Representation of UO_{2+x} ", J. Nucl. Mater. 130, 473-488 (1985).
4. NAKAMURA A. and T. FUJINO, "Thermodynamic Model of UO_{2+x} ", J. Nucl. Mater. 167, 36-46 (1989).
5. BESMANN T.M. and T.B. LINDEMNER, "Chemical Thermodynamic Representation of $\langle \text{PuO}_{2-x} \rangle$ and $\langle \text{U}_{1-z}\text{Pu}_z\text{O}_w \rangle$ ", J. Nucl. Mater. 130, 489-504 (1985).
6. MARTIN D.G., "A Re-Appraisal of the Thermal Conductivity of UO_2 and Mixed (U,Pu) Oxide Fuels", J. Nucl. Mater. 110, 73-94 (1982).

7. LUCUTA P.G., Hj. MATZKE and I.J. HASTINGS, "A Pragmatic Approach to Modelling Thermal Conductivity of Irradiated UO_2 Fuel: Review and Recommendations", *J. Nucl. Mater.* 232, 166-180 (1996).
8. AMAYA M. and M. HIRAI, "The Effects of Oxidation on the Thermal Conductivity of $(\text{U},\text{M})\text{O}_2$ Pellets ($\text{M} = \text{Gd}$ and/or Simulated Soluble FPs)", *J. Nucl. Mater.* 246, 158-164 (1997).
9. LINDNER R. and H. MATZKE, "The Diffusion of Xenon-133 in Uranium Oxide of Varying Oxygen Content", *Z. Naturforsch.* 14a, 582-584 (1959).
10. KILLEN J.C. and J.A. TURNBULL, "An Experimental and Theoretical Treatment of the Release of ^{85}Kr from Hyperstoichiometric Uranium Dioxide", *Proceedings of the Workshop on Chemical Reactivity of Oxide Fuel and Fission Product Release, Volume 2*, Eds. K.A. Simpson and P. Wood, CEGB, Berkeley, UK, 387-404 (1987).
11. UNE K., I. TANABE and M. OGUMA, "Effects of Additives and Oxygen Potential on the Fission Gas Diffusion in UO_2 Fuel", *J. Nucl. Mater.* 150, 93-99 (1987).
12. MANSOURI M.A. and D.R. OLANDER, "Fission Product Release from Trace Irradiated UO_{2+x} ", *J. Nucl. Mater.* 254, 22-33 (1998).
13. GRIMES R.W. and C.R.A. CATLOW, "The Stability of Fission Products in Uranium Dioxide", *Phil. Trans. Royal Soc. London*, A335, 609-634 (1994).
14. HOCKING W.H., A.M. DUCLOS and L.H. JOHNSON, "Study of Fission-Product Segregation in Used CANDU Fuel by X-Ray Photoelectron Spectroscopy (XPS) II", *J. Nucl. Mater.* 209, 1-26 (1994).
15. GRAPENGIESSER B. and D. SCHRIRE, "Impact of Systematic Stoichiometry Differences Among BWR Rods on Fission Gas Release", IAEA-TECHDOC-697, 103-110 (1992).
16. KLEYKAMP H., "The Chemical State of LWR High-Power Rods Under Irradiation", *J. Nucl. Mater.* 84, 109-117 (1979).
17. FLOYD M.R., J. NOVAK and P.T. TRUANT, "Fission-Gas Releases in Fuel Performing to Extended Burnups in Ontario Hydro Nuclear Generating Stations", Atomic Energy of Canada Limited Report, AECL-10636, 16 pages (1992).
18. BRADBURY B.T., J.T. DEMANT and P.M. MARTIN, "Solid Fission-Products in Irradiated Uranium Dioxide", *Proc. Brit. Ceram. Soc.* 7, 311-329 (1967).
19. BRAMMAN J.I., R.M. SHARPE, D. THOM and G. YATES, "Metallic Fission-Product Inclusions in Irradiated Oxide Fuels", *J. Nucl. Mater.* 25 201-215 (1968).
20. THOMAS L.E., C.E. BEYER and L.A. CHARLOT, "Microstructural Analysis of LWR Spent Fuels at High Burnup", *J. Nucl. Mater.* 188, 80-89 (1992).
21. LUCUTA P.G., R.A. VERRALL, Hj. MATZKE and B.J. PALMER, "Microstructural features of SIMFUEL — Simulated High-Burnup UO_2 -Based Nuclear Fuel", *J. Nucl. Mater.* 178, 48-60 (1991).
22. KLEYKAMP H., "Die Radiale Sauerstoff-Verteilung im Brennstoff Bestrahlter Mischoxid-Brennstabe Unterschiedlicher Ausgangsstoichiometrie", *J. Nucl. Mater.* 66, 292-300 (1977).
23. HASTINGS I.J., D.H. ROSE and J. BAIRD, "Identification of Precipitates Associated with Intergranular Fission Gas Bubbles in Irradiated UO_2 Fuel", *J. Nucl. Mater.* 61, 229-231 (1976).
24. NEWBURY D.E., D.C. JOY, P. ECHLIN, C.E. FIORI and J.I. GOLDSTEIN, "Advanced Scanning Electron Microscopy and X-Ray Microanalysis", Plenum, New York (1987).
25. GAULD I.C., "WOBI — An Integrated Two-Dimensional WIMS-AECL and ORIGEN-S Burnup Analysis Code System", Atomic Energy of Canada Limited Report, RC-1808 (1997).

26. BEHNKE R., L.C. BROWN and A.K. McILWAIN, "Performance of the WNRE Shielded SEM", Proceedings of the 2nd International Conference on CANDU Fuel, Ed. I.J. Hastings, Pembroke, Ontario, Canada, CNS, 282-291 (1989).
27. HE Z., D. ROSE, F. SZOSTAK, F.C. DIMAYUGA and M.H. SCHANKULA, "Quantitative WDS Analysis to Determine Plutonium Homogeneity in CANDU Mixed-Oxide Fuel", Proceedings of the 5th International Conference on CANDU Fuel, Ed. J.H. Lau, Toronto, Ontario, Canada, CNS, 279-288 (1997).
28. SMITH H.J., J.C. TAIT and R.E. VonMASSOW, "Radioactive Decay Properties of Bruce "A" CANDU UO₂ Fuel and Fuel Recycle Waste", Atomic Energy of Canada Limited Report, AECL-9072 (1987).
29. KLEYKAMP H., "Constitution and Thermodynamics of the Mo-Ru, Mo-Pd, Ru-Pd and Mo-Ru-Pd Systems", J. Nucl. Mater. 167, 49-63 (1989).
30. HOCKING W.H., A.M. DUCLOS, A.F. GERWING and K.M. WASYWICH, "Investigation of the Grain-Boundary Chemistry in Used CANDU Fuel by X-Ray Photoelectron Spectroscopy (XPS)", International Atomic Energy Agency Report, IAEA-TECHDOC-822, 223-240 (1995).
31. HOCKING W.H., R. BEHNKE, A.M. DUCLOS, A.F. GERWING and P.K. CHAN, "Investigation of the CANLUB/Sheath Interface in CANDU Fuel at Extended Burnup by XPS and SEM/WDX", Proceedings of the 5th International Conference on CANDU Fuel, Ed. J.H. Lau, Toronto, Ontario, Canada, CNS, 376-392 (1997).
32. JAIT J.C., I.C. GAULD and G.B. WILKIN, "Derivation of Initial Radionuclide Inventories for the Safety Assessment of the Disposal of Used CANDU Fuel", Atomic Energy of Canada Limited Report, AECL-9881 (1989).
33. FUJINO T., "Thermodynamics of Fluorite Type Solid Solutions Containing Plutonium, Lanthanide Elements or Alkaline Earth Metals in Uranium Dioxide Host Lattices", J. Nucl. Mater. 154, 14-24 (1988).
34. PARK K., "The Oxygen Potential of Neodymia-Doped Urania Based on a Defect Structure", J. Nucl. Mater. 209, 259-262 (1994).
35. FUJINO T., N. SATO and K. YAMADA, "A Refined Analysis of Oxygen Potential of M_yU_{1-y}O_{2+x} (M = M³⁺ and M²⁺) by Lattice Statistics Based on the Grand Partition Function and the Flory Methods", J. Nucl. Mater. 223, 6-19 (1995).
36. IMOTO S., "Chemical State of Fission Products in Irradiated UO₂", J. Nucl. Mater. 140, 19-27, (1986).
37. CORDFUNKE E.H.P. and R.J.M. KONINGS, "Chemical Interactions in Water-Cooled Nuclear Fuel: A Thermodynamic Approach", J. Nucl. Mater. 152, 301-309 (1988).
38. UNE K., "Reactions of Cesium with Nonstoichiometric UO_{2+x} and U_{0.86}Gd_{0.14}O_{2+x} Pellets", J. Nucl. Mater. 144, 128-140 (1987).
39. McEACHERN R., "Oxidation Behaviour of Noble-Metal Inclusions in Used UO₂ Nuclear Fuel", Atomic Energy of Canada Limited Report, AECL-11818 (1997).
40. COX B., "Pellet-Clad Interaction (PCI) Failures of Zirconium Alloy Fuel Cladding — A Review", J. Nucl. Mater. 172, 249-292 (1990).
41. MATZKE H.J., "Atomic Transport Properties in UO₂ and Mixed Oxides (U,Pu)O₂", J. Chem. Soc. Faraday Trans. 2, 1121-1142 (1987).
42. SARI C. and G. SCHUMACHER, "Oxygen Redistribution in Fast Reactor Oxide Fuel", J. Nucl. Mater. 61, 192-202 (1976).

TABLE 1. POWER HISTORIES AND SELECTED PIE DATA FOR FUELS IN WHICH THE NOBLE-METAL PARTICLES WERE ANALYZED BY WAVELENGTH DISPERSIVE X-RAY (WDX) MICROANALYSIS.

Fuel Bundle	Element Number	Burnup (MW·h/kg U)	Peak Power (kW/m)	Power Profile	Fission-Gas Release (%)	CANLUB Retention (%)
P11171W ¹	7	204	50	Constant	5.3	NM ⁵
J98315C ²	28	472	47	Declining	4.6	63
J03311W ²	3	544	59	Declining	24	62
BDL-406-GF ³	1,2	950	37	Constant	17	20
BDL-419-ABC ⁴	1	520	59	Declining	12	52

¹Natural UO₂ fuel irradiated as a 28-element bundle in Pickering NGS-A.

²Natural UO₂ fuel irradiated as a 37-element bundle in Bruce NGS-A.

³Natural UO₂ fuel irradiated as a Bruce-type bundle in NRU.

⁴Mixed oxide (MOX) fuel, with 0.55% Pu in natural UO₂, irradiated as a Bruce-type bundle in NRU.

⁵Not measured, but other elements with a similar burnup typically show an essentially complete CANLUB layer.

TABLE 2. CALCULATED RELATIVE PROPORTIONS OF NOBLE METALS IN IRRADIATED NATURAL UO₂ FUELS STUDIED BY X-RAY MICROANALYSIS.

Fuel	Mo (wt.%)	Tc (wt.%)	Ru (wt.%)	Rh (wt.%)	Pd (wt.%)	Mo/Ru (ratio)	Mo/Pd (ratio)
P11171W/7 ¹	39.4	10.0	26.1	8.0	16.5	1.51	2.39
J98315C/28 ²	35.7	9.1	28.2	6.5	20.4	1.27	1.75
J03311W/3 ²	35.0	8.9	28.4	6.2	21.5	1.23	1.63
406-GF/1 ²	32.4	7.4	28.0	3.7	28.5	1.16	1.14

¹Derived from noble-metal inventories determined by interpolation between tabulated data for CANDU power reactor fuel [28].

²Derived from noble-metal inventories calculated from the fuel power history using the WIMS-ORIGEN program [25].

TABLE 3. MEASURED COMPOSITION OF NOBLE-METAL PARTICLES IN J03311W/3

Particle Number	Mo (wt.%)	Tc (wt.%)	Ru (wt.%)	Rh (wt.%)	Pd (wt.%)	Mo/Ru (ratio)	Mo/Pd (ratio)
1	34.7	11.4	33.2	4.2	16.5	1.04	2.10
2	34.4	10.2	31.7	7.3	16.4	1.08	2.10
3	34.7	11.2	31.8	5.1	17.2	1.09	2.02
4	33.9	10.8	32.3	6.5	16.5	1.05	2.05
5	33.3	11.0	32.1	6.1	17.5	1.04	1.90
6	33.7	11.1	32.6	5.9	16.7	1.03	2.02
7	33.9	11.7	35.0	5.0	14.4	0.97	2.35
8	34.0	11.7	34.2	5.9	14.2	0.99	2.39
9	37.6	9.9	29.8	5.3	17.4	1.26	2.16
10	32.8	14.2	28.0	5.8	19.2	1.17	1.71
11	30.3	9.1	27.0	6.6	27.0	1.12	1.12
12	29.2	8.3	27.9	10.3	24.3	1.05	1.20
Average (1-8)	34.1(2) ¹	11.1(2) ¹	32.9(4) ¹	5.8(3) ¹	16.2(4) ¹	1.04(1) ¹	2.12(6) ¹
Average (1-12)	33.5(6) ¹	10.9(4) ¹	31.3(7) ¹	6.2(4) ¹	18.1(11) ¹	1.07(2) ¹	1.93(11) ¹

¹Standard deviation of the mean in units of the least significant figure.

TABLE 4. MEASURED Mo/Ru AND Mo/Pd RATIOS FOR THREE IRRADIATED FUELS

Particle Number	J98315C/28		BDL-406-GF/1		BDL-419-ABC/1	
	Mo/Ru (ratio)	Mo/Pd (ratio)	Mo/Ru (ratio)	Mo/Pd (ratio)	Mo/Ru (ratio)	Mo/Pd (ratio)
1	1.15	2.33	1.15	2.24	1.40	3.00
2	1.23	1.73	1.16	2.80	1.13	2.42
3	1.33	2.30	1.07	2.76	1.14	2.51
4	1.39	2.36	1.22	1.59	1.05	2.22
5	1.18	2.44	1.12	1.54	0.99	2.08
6	1.36	3.92	1.17	2.24	1.31	1.47
7	1.26	2.66	1.23	2.05	0.97	0.31
8			1.51	2.01	1.02	0.01
Average (1-6)					1.17(6) ¹	2.28(21) ¹
Average (1-7)	1.27(4) ¹	2.53(25) ¹	1.16(2) ¹	2.17(19) ¹		
Average (1-8)			1.20(5) ¹	2.15(16) ¹		

¹Standard deviation of the mean in units of the least significant figure.

TABLE 5. EXPECTED VALENCE STATE OF FISSION PRODUCTS IN CANDU FUEL

Valence State	ΔG_{O_2} Below MoO_2/Mo Boundary	ΔG_{O_2} Above MoO_2/Mo Boundary
+5		Nb
+4	Zr, Nb, Ce	Zr, Ce, Mo, Sn
+3	Y, La, Pr, Nd, Pm, Sm, Eu, Gd, Tb, Dy, Ho, Er	Y, La, Pr, Nd, Pm, Sm, Eu, Gd, Tb, Dy, In, Ho, Er
+2	Sr, Ba	Sr, Ba
+1	Rb, Cs	Rb, Cs
0	As, Ge, Se, Kr, Mo, Tc, Ru, Rh, Pd, Ag, Cd, In, Sn, Sb, Te, Xe	As, Ge, Se, Kr, Tc, Ru, Rh, Pd Ag, Cd, Sb, Te, Xe
-1	Br, I	Br, I

TABLE 6. OXYGEN BALANCE IN CANDU FUELS WITH NORMAL AND HIGH BURNUP

Oxygen Sources ¹ and Sinks ²	Bruce A Fuel (190 MWh/kg U)		BDL-406-GF (950 MWh/kg U)	
	mmole O per mole Actinide	mmole O per Element	mmole O per mole Actinide	mmole O per Element
Fission-Freed O				
Mo as MoO_2	-0.33	-0.70	9.80	20.1
Mo Elemental	3.20	6.83	32.9	67.3
Intrinsic O Sinks				
$RE_yU_{1-y}O_2$	1.44	3.08	9.05	18.5
$AE_yU_{1-y}O_{2-z}$	$\alpha(1.20)$	$\alpha(2.57)$	$\alpha(6.17)$	$\alpha(12.6)$
$(Cs,Rb)_2UO_{4-z}$	$\beta(0.66)$	$\beta(1.42)$	$\beta(3.09)$	$\beta(6.33)$
SnO_2, CdO, TeO_2	$\gamma(0.49)$	$\gamma(1.05)$	$\gamma(4.10)$	$\gamma(8.39)$
Extrinsic O Sinks				
CANLUB H	$\delta(0.9)$	$\delta(2)$	$\delta(1)$	$\delta(2)$
CANLUB C	$\eta(7.8)$	$\eta(16.7)$	$\eta(8.1)$	$\eta(16.7)$
ZrO ₂ Film			2.6	5.3
Zr Dissolution			?	?

¹Amount of oxygen released by fission derived from calculated fission-product inventories [25,32] assuming valence states listed in Table 5.

²Coefficients allow for less than maximum possible consumption of oxygen by sinks, i.e., α , β , γ , δ and η should all have values of less than 1 (see text).

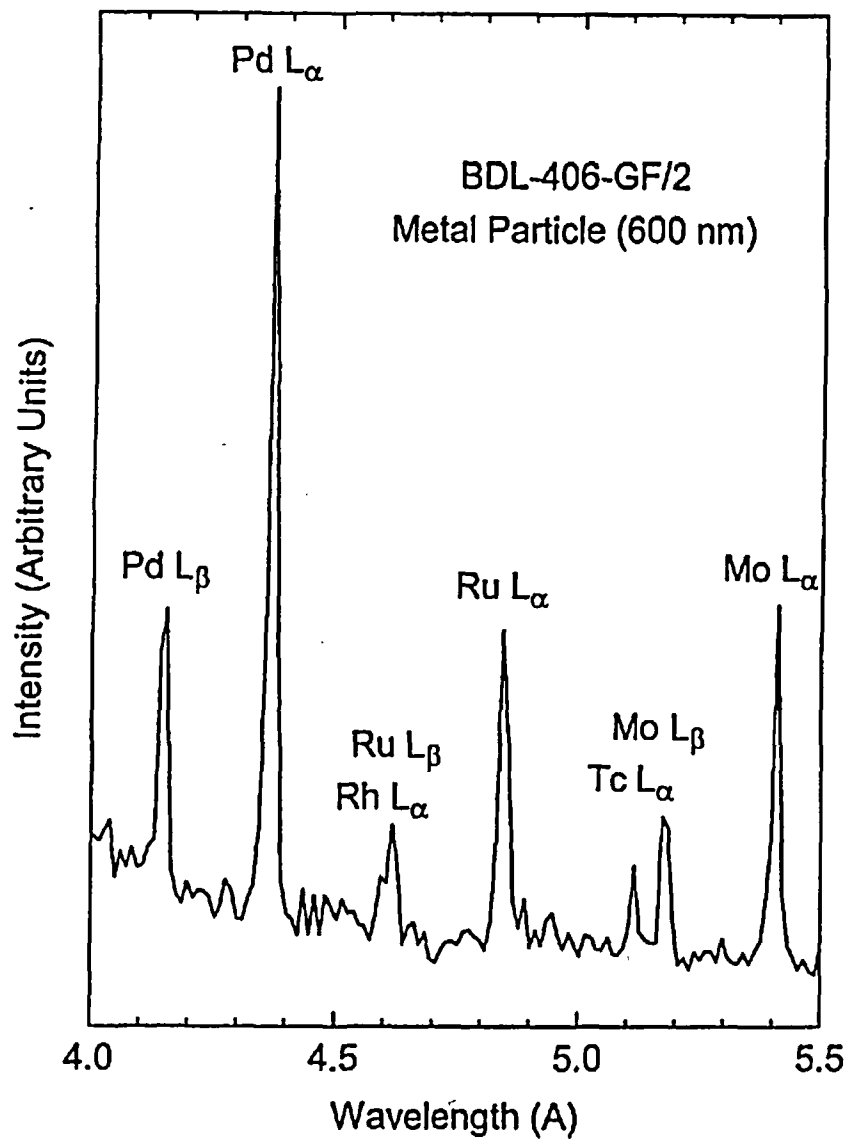


FIGURE 1. WDX SPECTRUM RECORDED FROM PARTICLE IN HIGH-BURNUP CANDU FUEL

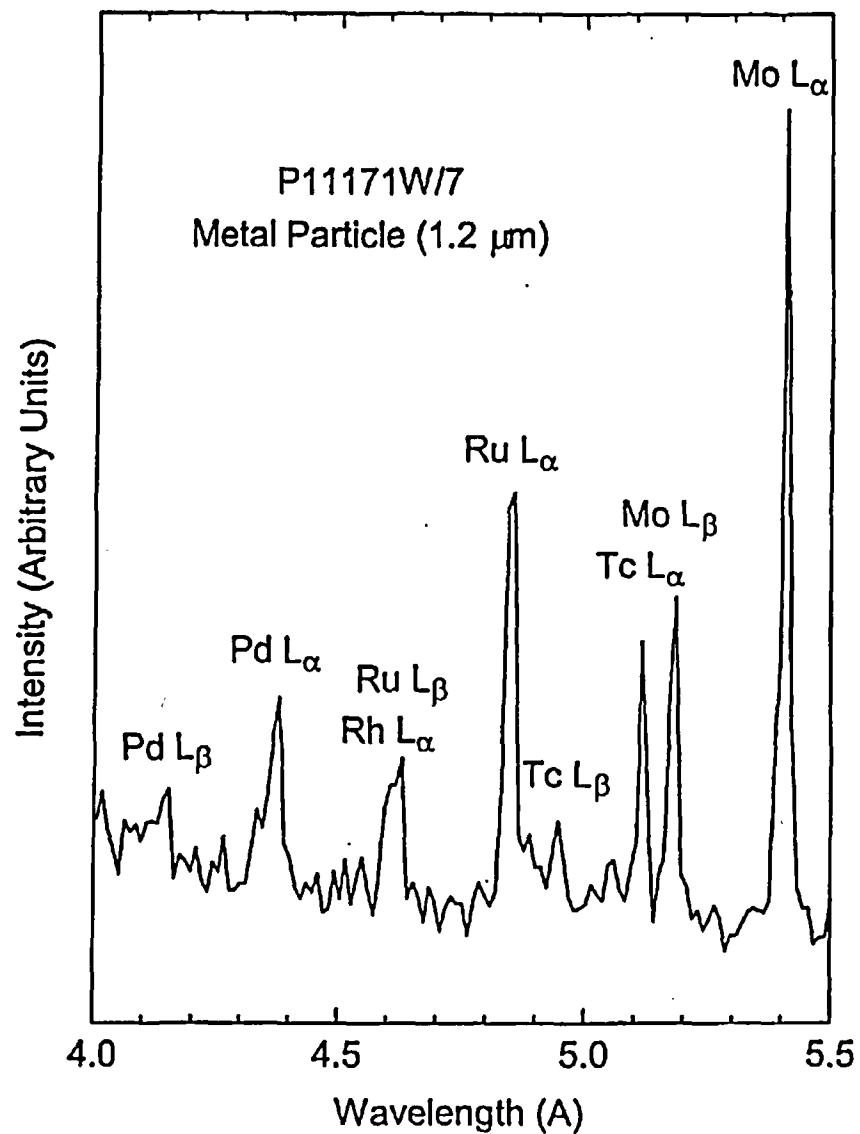


FIGURE 2. WDX SPECTRUM RECORDED FROM PARTICLE IN NORMAL-BURNUP CANDU FUEL

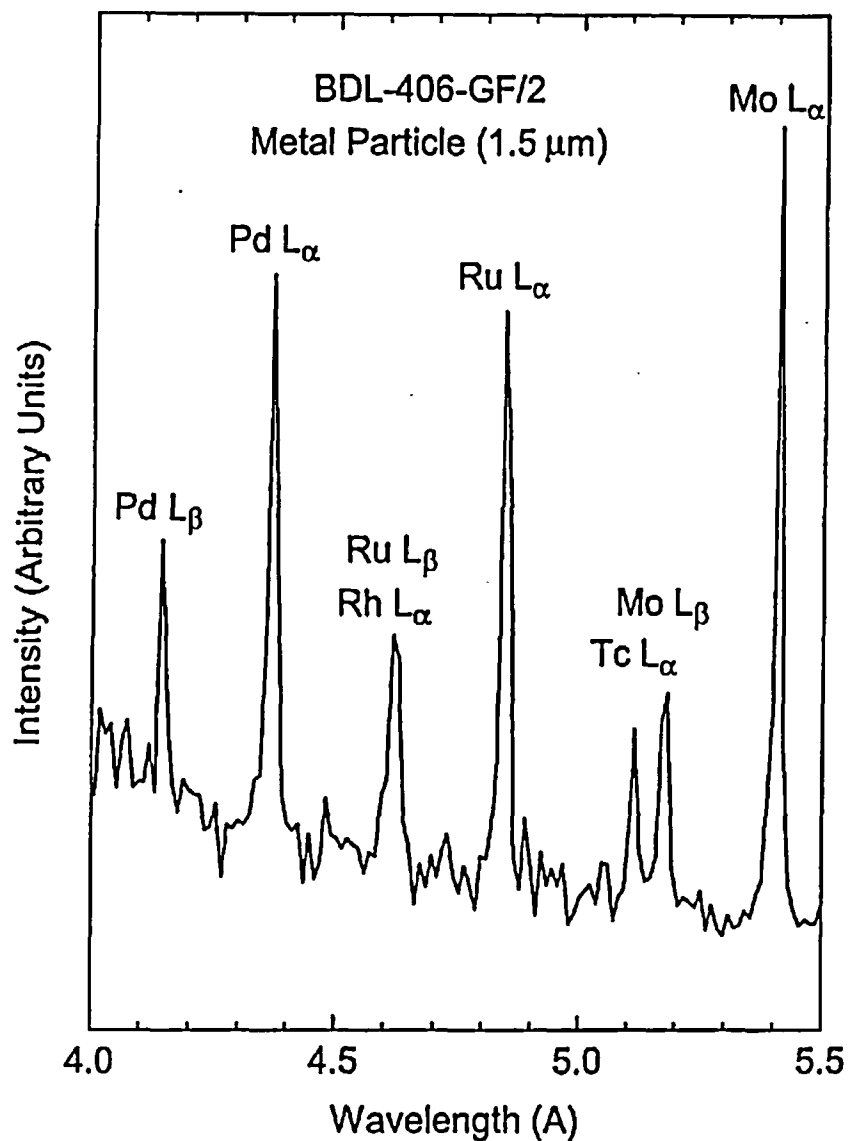


FIGURE 3. WDX SPECTRUM RECORDED FROM PARTICLE IN HIGH-BURNUP CANDU FUEL

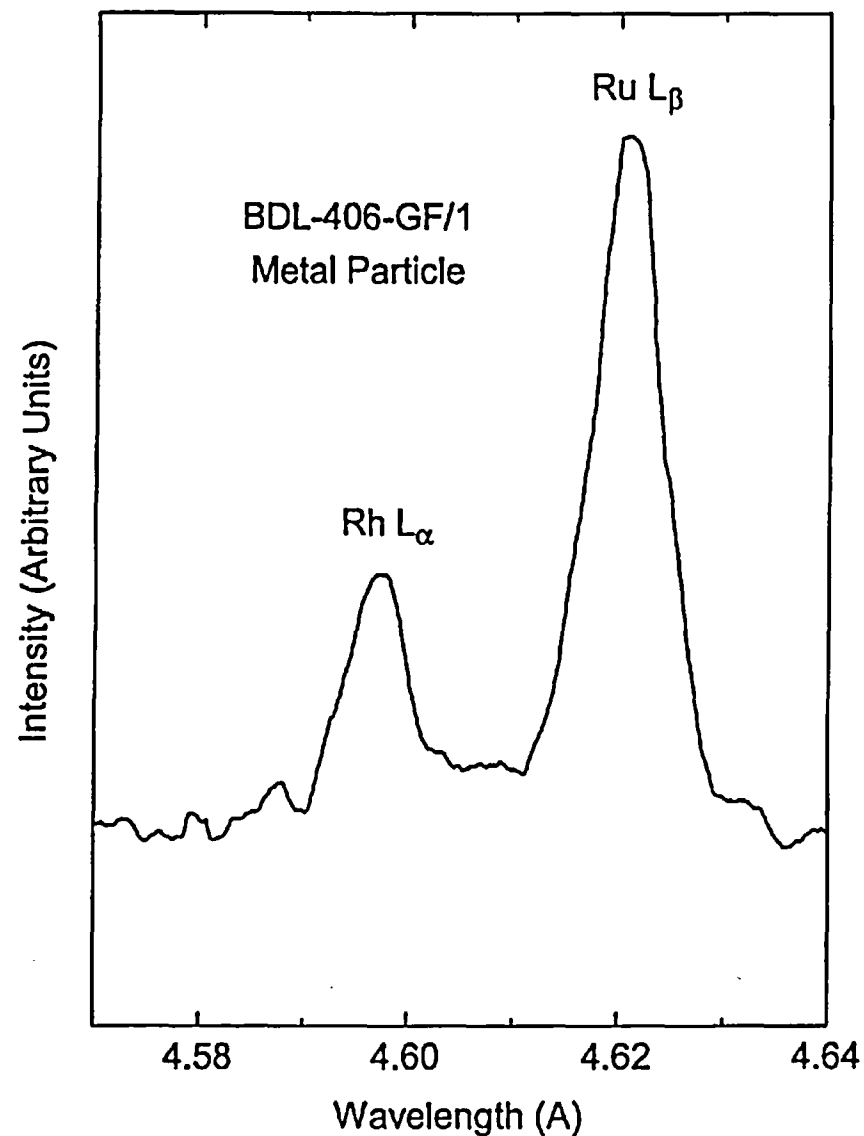


FIGURE 4. WDX SPECTRUM RECORDED FROM PARTICLE IN HIGH-BURNUP CANDU FUEL